Исследование нейтроно-дефицитных изотопов висмута методом спектроскопии в лазерном ионном источнике (ИРИС, ISOLDE)

П.Л. Молканов,

А.Е. Барзах,
В.Н. Пантелеев,
Д.В. Федоров,
М.Д. Селиверстов,
В.С. Иванов,
С.Ю. Орлов,
Ю.М. Волков

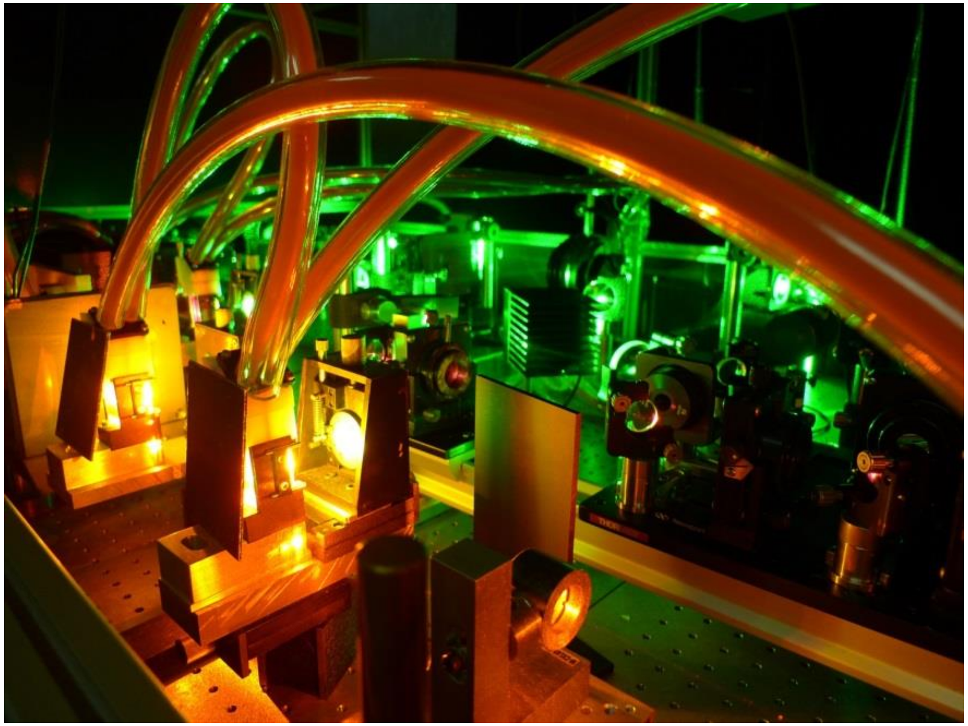

НИЦ «Курчатовский институт» - ПИЯФ, семинар ОФВЭ

14/12/2021

Laser spectroscopy in nuclear physics

High-resolution laser spectroscopy is been established as a powerful tool in the study of nuclear shape, size and nuclear moments.

Deduced **nuclear parameters** are:

- ✓ changes in the mean-square charge radius $\delta\langle r^2\rangle$
- ✓ electric quadrupole moment Q_s
- ✓ nuclear spin I
- ✓ magnetic dipole moment μ

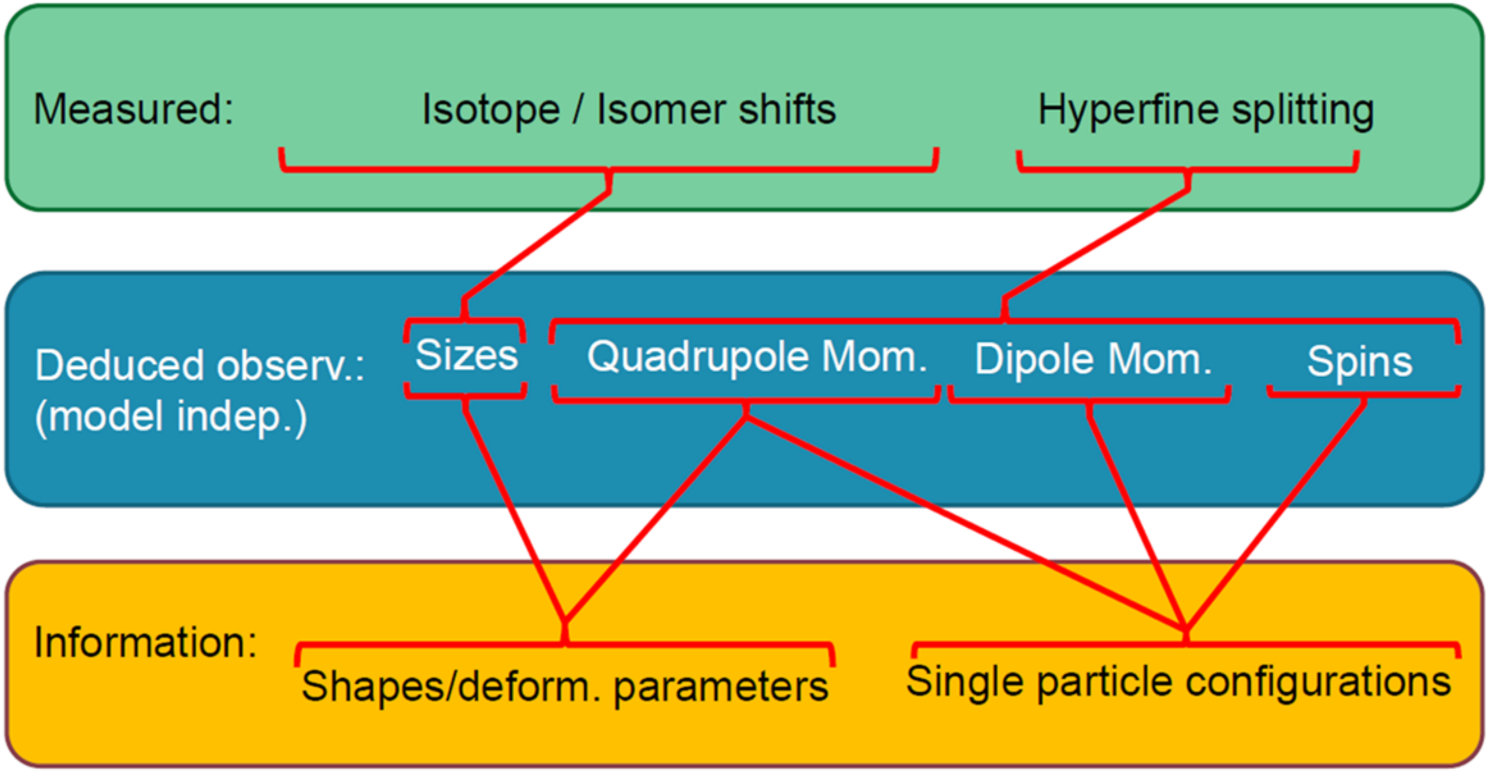

Nuclear charge radius and Nuclear deformation

$$\langle r^2\rangle = \frac{\int_0^\infty \rho(\vec{r})\, r^2 d^3r}{\int_0^\infty \rho(\vec{r})\, d^3r}$$ mean-square nuclear charge radius (*mscr*)

$$\langle r^2\rangle \approx \langle r^2\rangle_0 \left(1 + \frac{5}{4\pi}\langle \beta_2^2\rangle\right)$$

$<r^2>_0$ - *mscr* of a spherical nucleus of identical volume

$<\beta_2>$ - quadrupole deformation parameter

$\delta<r^2>^{A,A'}$ - the change in *mscr* between the two isotopes

Influence of the nuclear deformation on changing of charge radii:

$$\delta\langle r^2\rangle^{A,A'} = \delta\langle r^2\rangle_0^{A,A'} + \langle r^2\rangle_0 \cdot \frac{5}{4\pi}\delta\langle \beta_2^2\rangle^{A,A'}$$

Spherical shape:
$\langle\beta_2\rangle = 0$

Prolate deformed shape:
$\langle\beta_2\rangle > 0$

Oblate deformed shape:
$\langle\beta_2\rangle < 0$

$\delta<r^2>$ is very sensitive to changes in the nuclear shape

Addition of a neutron at $A \sim 100$:

- ✓ spherical nuclear shape $\langle\beta_2^2\rangle = 0.0$
- ✓ deformed nuclear shape $\langle\beta_2^2\rangle = 0.1$

⇒

$\delta\langle r^2\rangle \sim 0.07$ fm^2

$\delta\langle r^2\rangle \sim 0.74$ fm^2

Main isotopic trend of *mscr* is described by the Droplet Model. Deviations from the DM trend are attributed to the advance of the mean-square quadrupole deformation

Pioneering experiments in Pb-region (Z = 82)

The shape and the size of a nucleus are among its most fundamental properties.
Usually, isotopic dependence of nuclear radii is smooth,
however, at the certain neutron numbers there are marked irregularities.

Isotope shift (IS) measurements in the lead region of
$^{177-186}$Hg (Z = 80) near the neutron mid-shell at N = 104

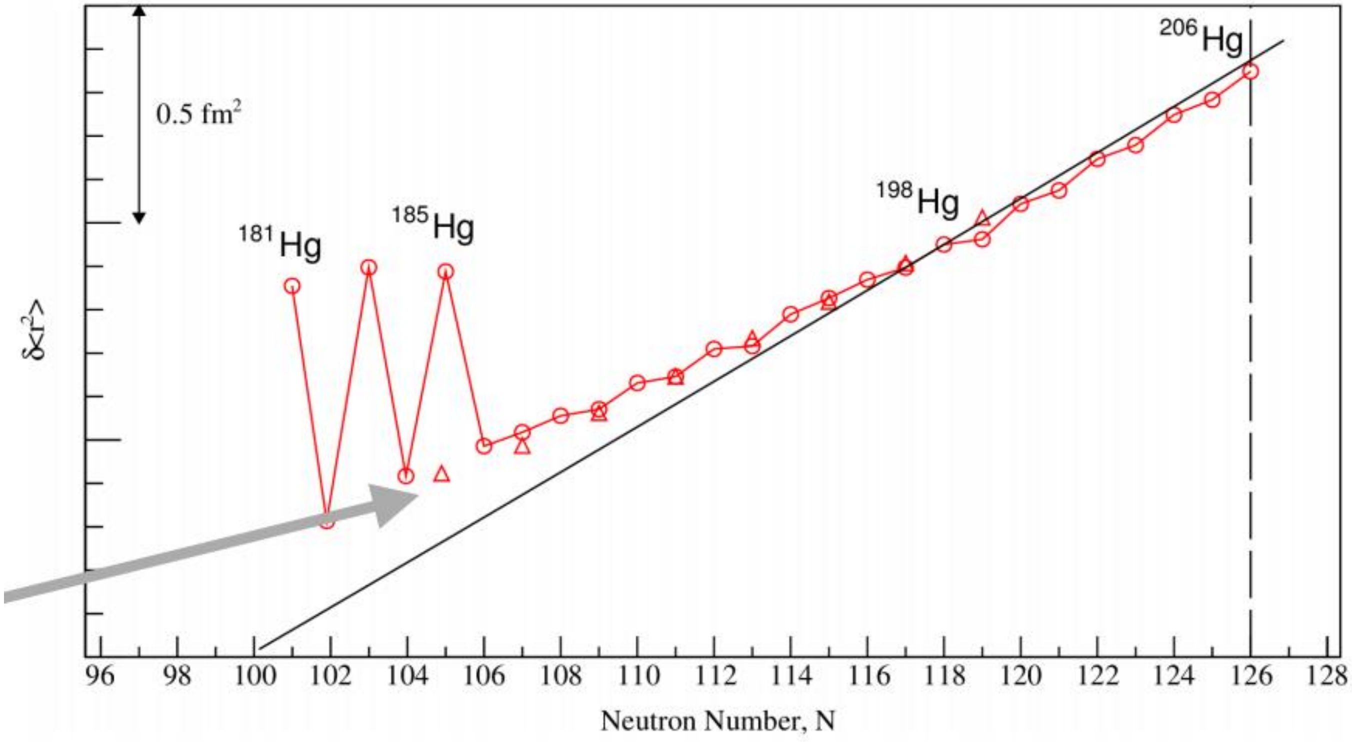

J. Bonn, G. Huber, H.-J. Kluge, L. Kugler, and E. Otten,
Phys. Lett. B **38**, 308 (1972).

This phenomenon was characterized as
“one of the most remarkable discoveries in nuclear structure physics in the last 50 years”.

K. Heyde and J. L. Wood, Phys. Scripta 91, 083008 (2016)

Motivation for the optical spectroscopy in Pb-region

Interpretation:

Sharp changes between nearly spherical shapes in the even-A cases and strongly-prolate deformed configurations in the odd-A isotopes

Assumption:

The neutron-deficient isotopes near Z = 82 (Pb-region) exhibit the richest manifestation of shape evolution and shape coexistence phenomena

Experimental tasks:

✓ to extend of mercury measurements down to ^{180}Hg and beyond

✓ to investigate the ground and isomeric states shapes for different elements in Pb-region

Experimental challenge

The center of Pb-region lies far from stability:

✓ low production cross sections
✓ overwhelming production of isobaric contaminants
✓ very short half lives of most nuclei of interest

Conclusion

For experimental investigations in Pb-region should be used the most extreme methods ever developed for far-from-stability nuclear structure study

Solution

✓ Measurements at ISOL facilities *(ISOL = Isotope Separator On-Line)*

- large production yield rates from the thick targets
- ionization enhancement in *laser ion source* (LIS)
- isobaric selectivity in LIS what is crucial for far-from-stability studies

✓ Using of the optical spectroscopy techniques as very sensitive tool

Nuclear shape staggering

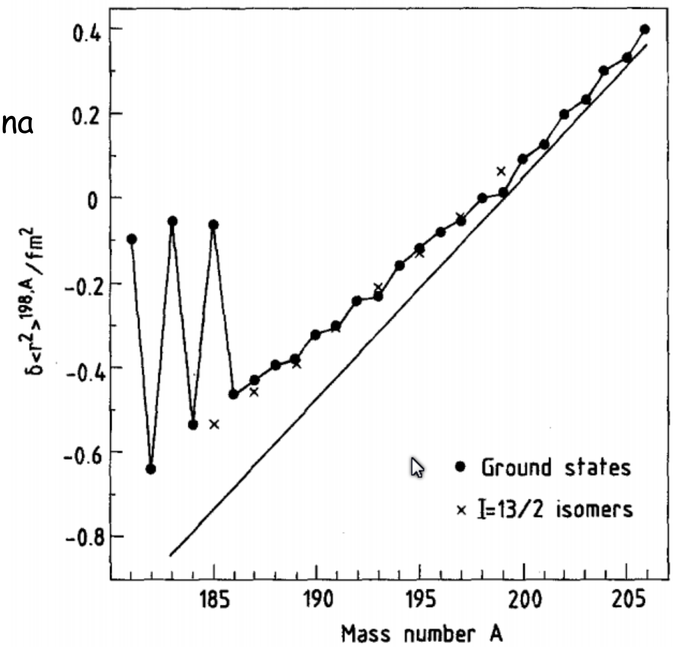

"The extension of these measurements down to ^{180}Hg might be made feasible by improving experimental details. It could thus be determined whether the shape staggering extends further, and where the nuclear shape becomes stabilized finally".

J. Bonn, G. Huber, H.-J. Kluge, L. Kugler, and E. Otten, Phys. Lett. 38B, 308 (1972)

Ion beam production at ISOL facilities

ISOL technique step-by-step:

- ✓ Production of the radioactive isotopes in target
- ✓ Ionization in hot cavity
- ✓ Extraction from the target-ion source system
- ✓ Mass separation
- ✓ Transport to experimental setups

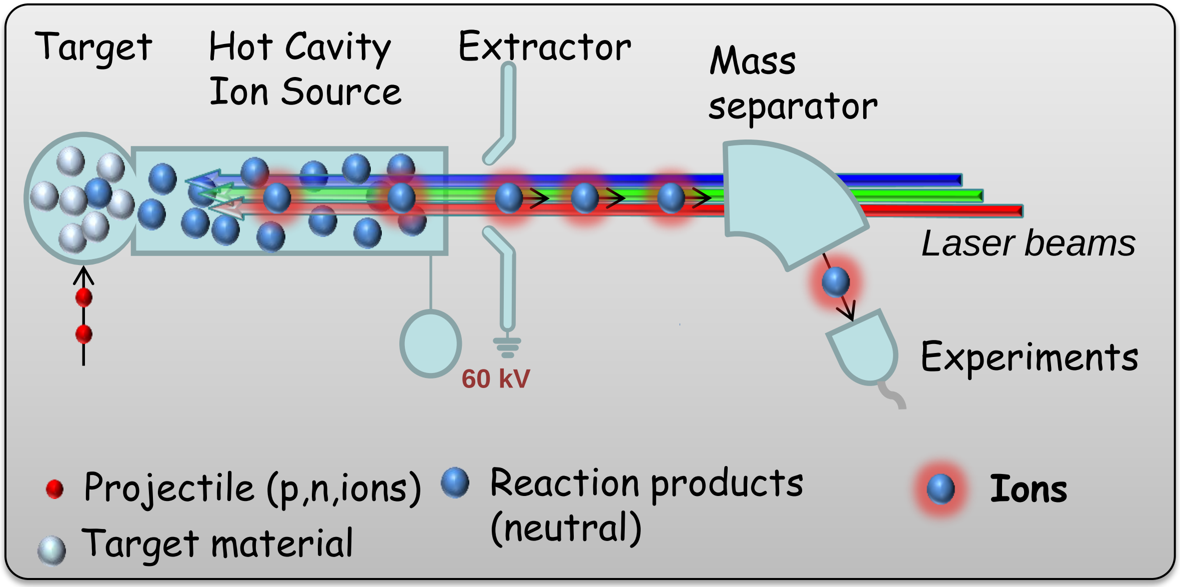

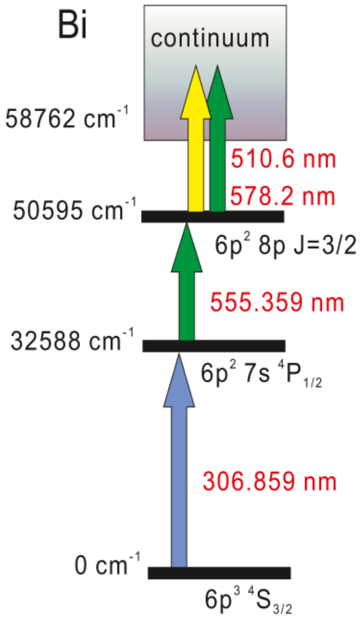

Benefits	Drawbacks
large production yield rates from the thick targets	slow release of the some radioactive products from the target matrix, some elements are irreversibly trapped
efficient surface ionization (for alcali), efficient laser ionization (for volatile)	surface ionization of isobaric contaminants => limited purity of RIB

Laser ion source: ionization efficiency

Ionization in a hot cavity:

The hot cavity concept has been developed with the goal of increasing the ionization efficiency of atoms moving in a vacuum through pulsed laser beams.

The geometry of the cavity provides confinement of atoms within the laser beam during the time interval between consecutive laser pulses while the hot environment prevents atoms from absorption on the cavity internal walls.

Schematic drawing of the hot cavity LIS

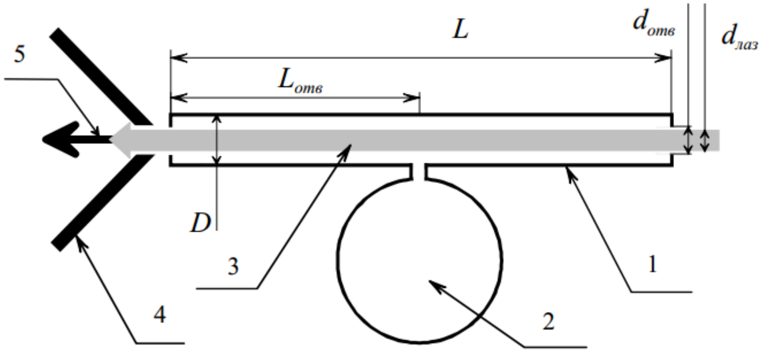

1 – ionization cavity; 2 - target; 3 - laser beams;
4 - extractor; 5 - ion beam

Due to its high efficiency (usually ~10%) *Laser Ion Source* is very appropriate at ISOL facilities for:

- ✓ radioactive ion beam production
- ✓ atomic and nuclear spectroscopy

of rare isotopes produced in very small quantities (less than 1 ion/s)

Experimental alpha-spectra collected in "laser-on" and "laser-off" regimes

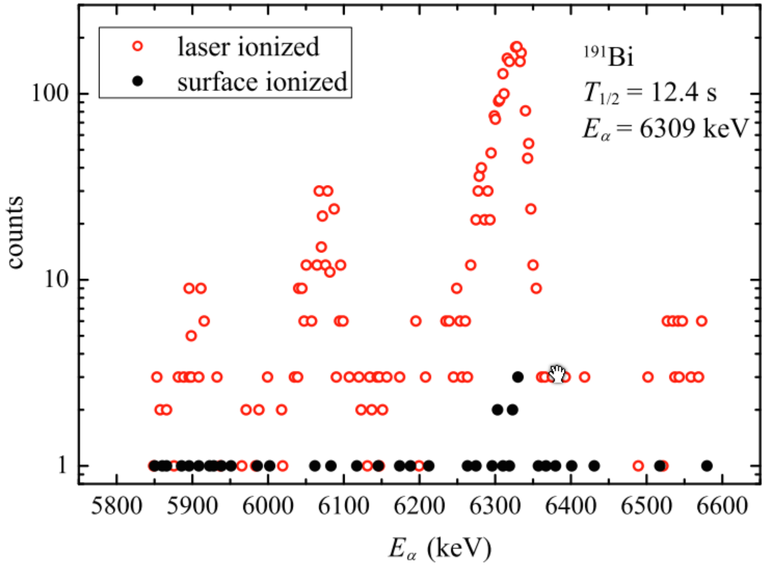

Laser ion source: selectivity

$$Selectivity = \frac{I_{\Sigma}}{I_{bgr}}$$

isobar selectivity after ***Laser IS***

Isotope of interest

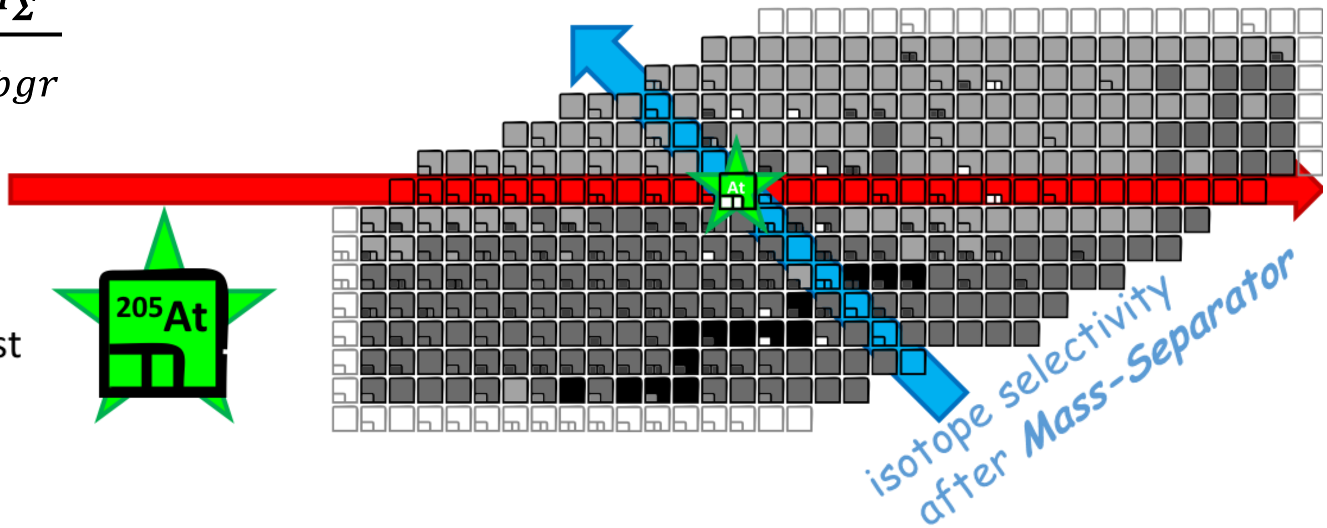

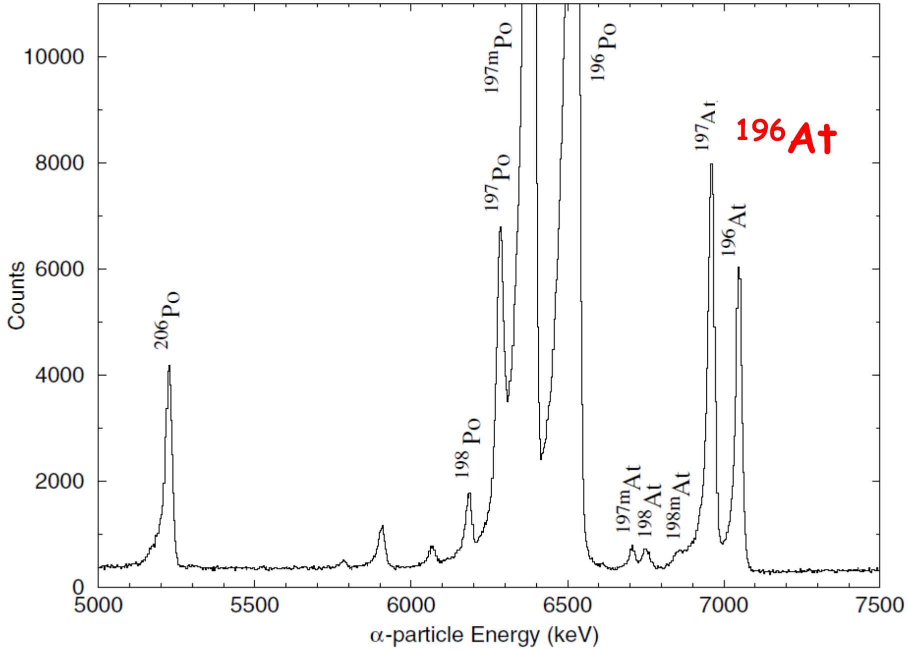

RITU: M.B. Smith et al., J. Phys. G. 26, 787 (2000)

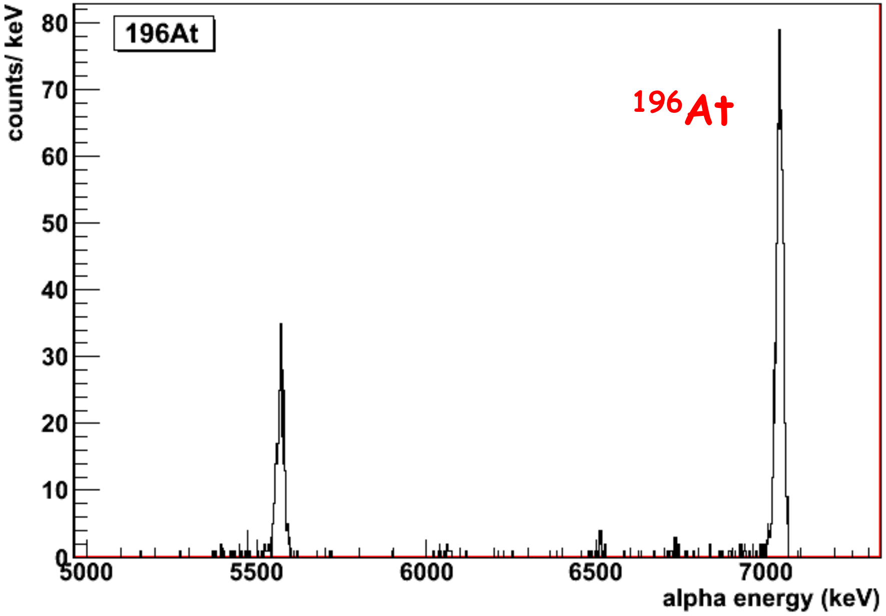

RILIS + ISOLDE (IS534)

Method of resonance laser ionization

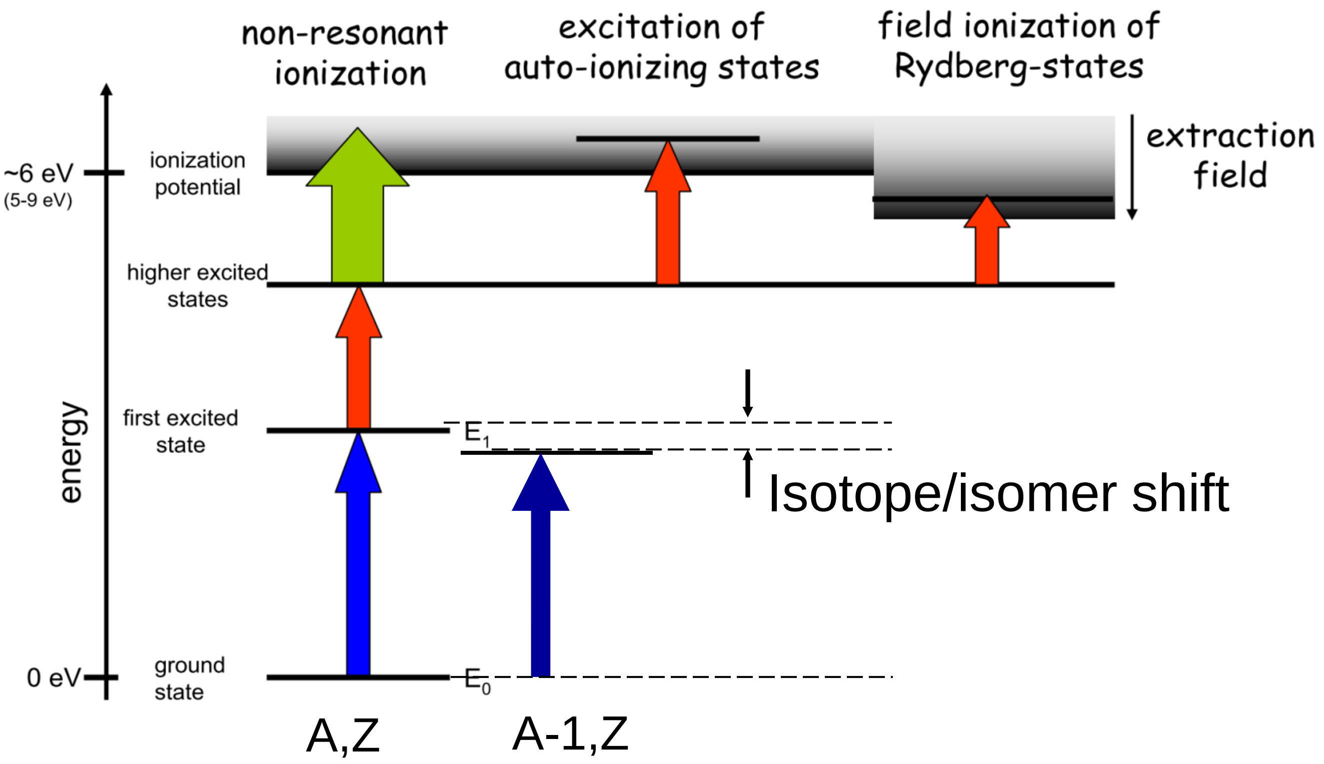

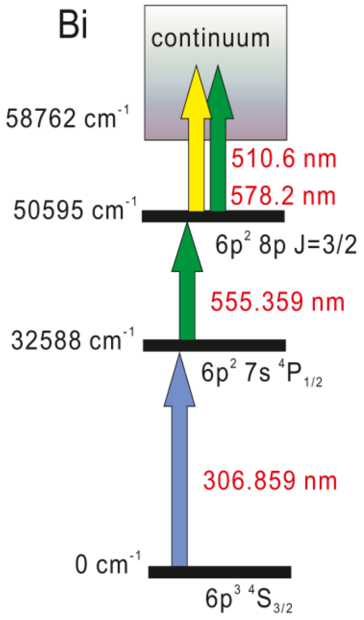

Isotope shift (IS), hyperfine structure (HFS) measurements:

By scanning the narrow-band laser frequency over the resonance, together with simultaneous counting of the mass-separated photo-ions, the **isotope shifts** and **hyperfine structure** of the atomic spectral lines can be measured

Laser installation of the IRIS facility (since 2009)

Scheme of IRIS Laser Installation

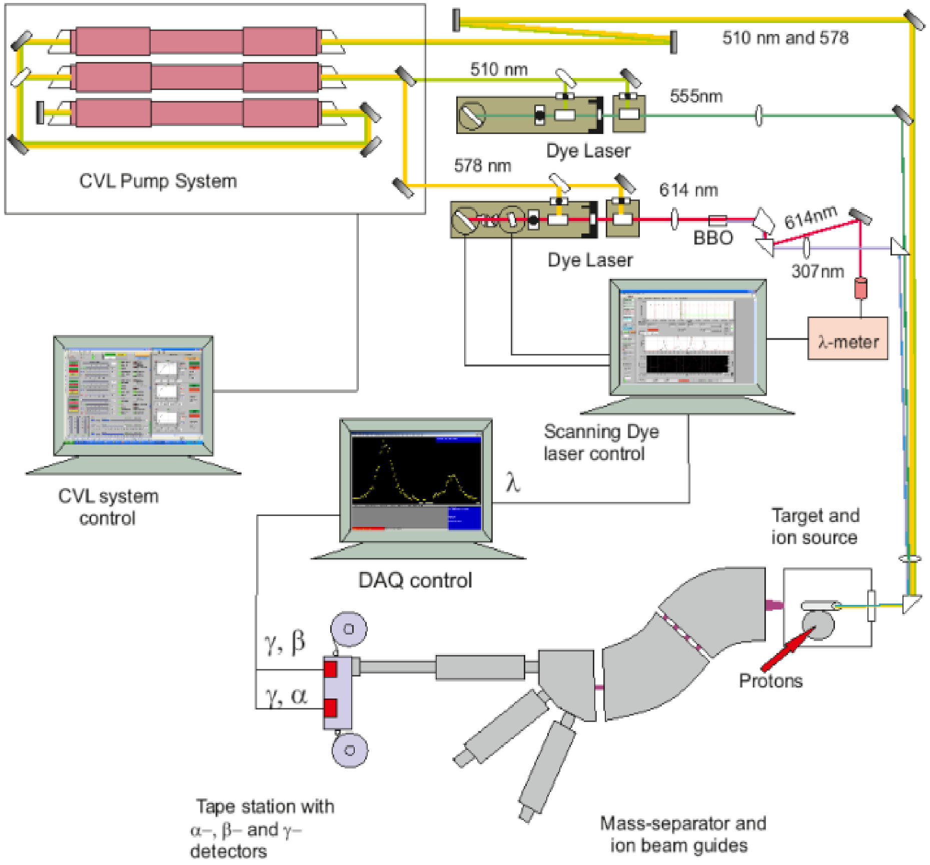

IRIS Laser Installation

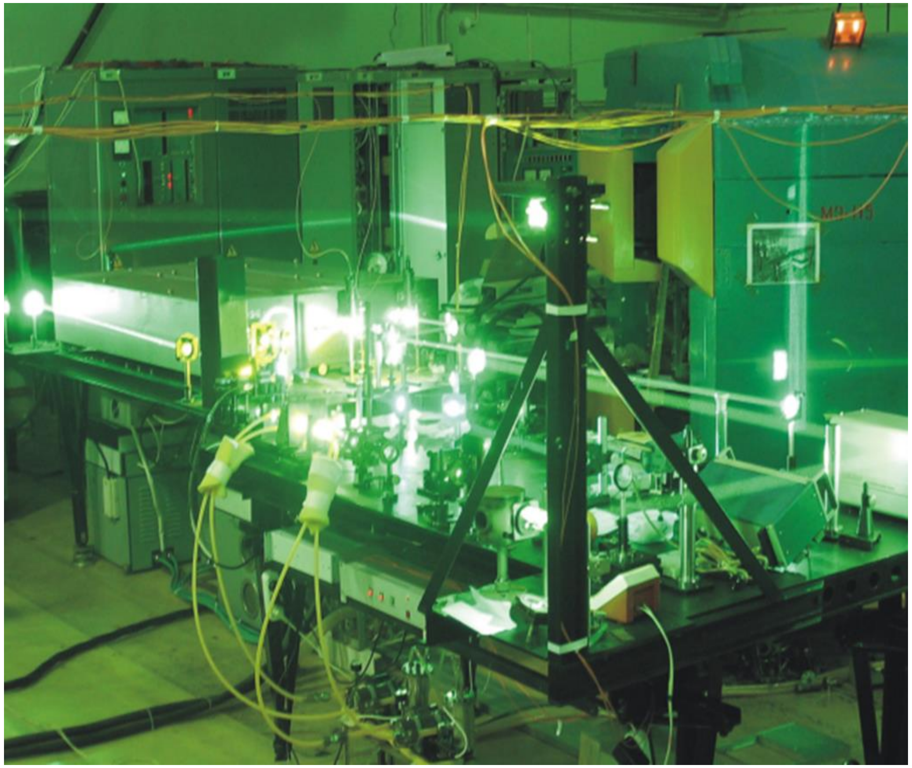

Spectral range: 530 – 850 nm,
after doubling: 265 – 850 nm

Charge radii in the lead region (2003)

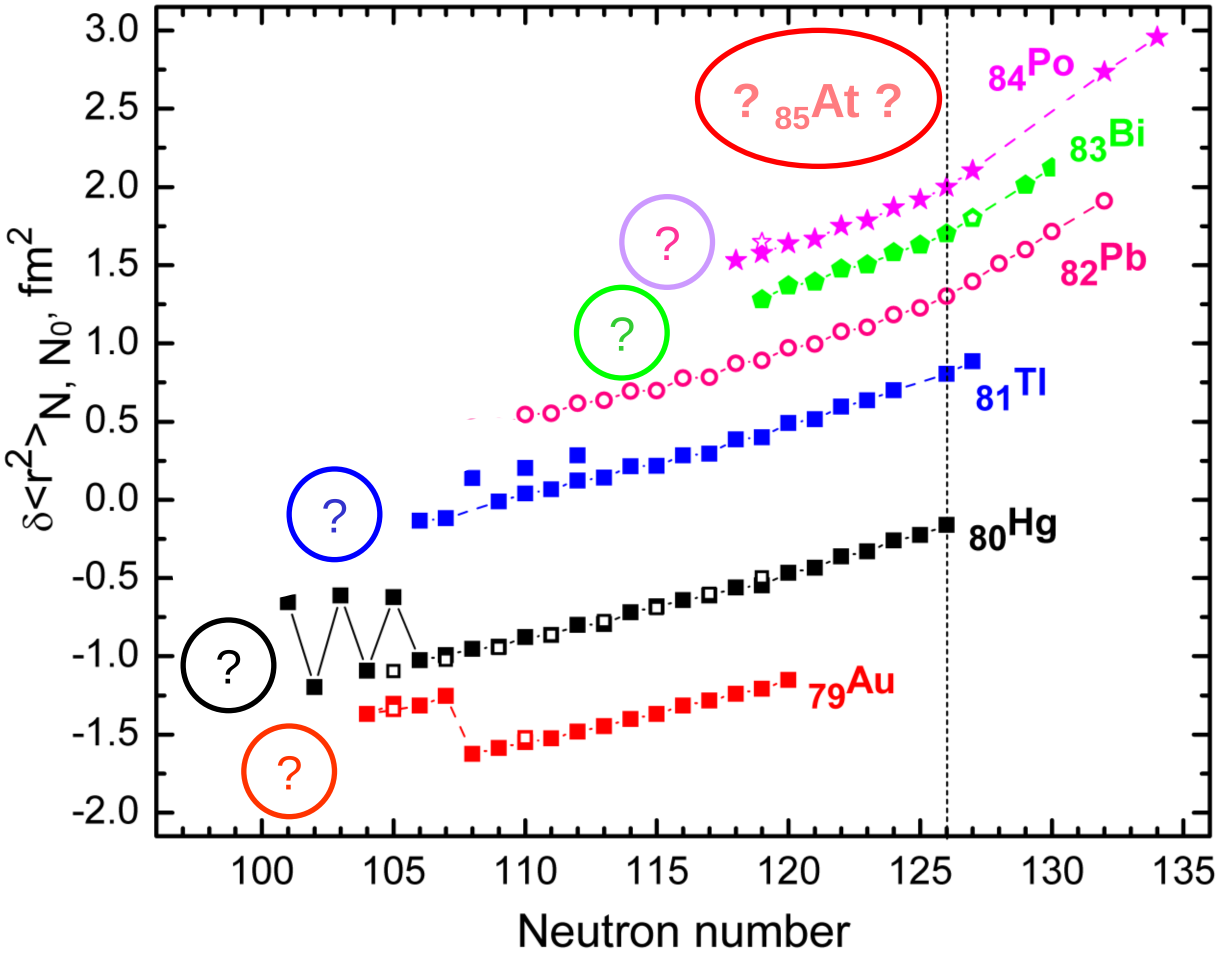

IRIS, Bi: radii

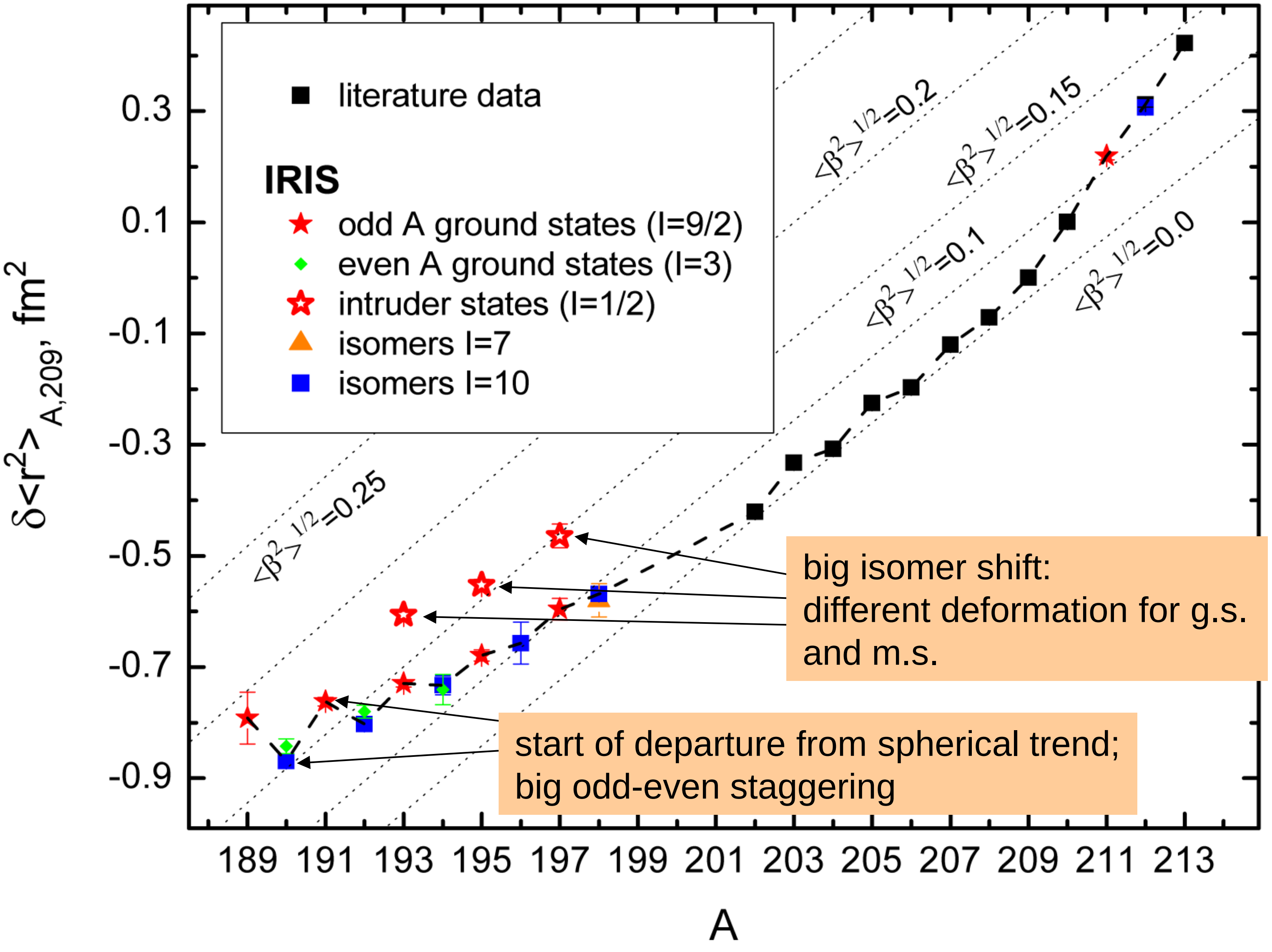

big isomer shift:
different deformation for g.s.
and m.s.

start of departure from spherical trend;
big odd-even staggering

Windmill-ISOLTRAP-RILIS collaboration at ISOLDE (CERN)

IS 456, 466, 511, 534, 598, 608:

Laser spectroscopy: shape evolution and shape-coexistence studies with radioactive $_{79}$Au, $_{80}$Hg, $_{81}$Tl, $_{82}$Pb, $_{83}$Bi, $_{84}$Po, $_{85}$At beams

- A collaboration of ~40 atomic and nuclear physicists
- 15 institutions

IS608 Experiment @ ISOLDE

IS608
Shape-coexistence and shape-evolution studies for bismuth isotopes by in-source laser spectroscopy and beta-delayed fission in ^{188}Bi

IS608 laser spectroscopy goals:

1) Onset of deformation investigation
   by re-measuring a somewhat uncertain data for ^{189}Bi from IRIS and measuring ^{187}Bi (N=104), for which this effect is expected to be maximized;
2) Investigation of the strong odd-even staggering to at least ^{187,188}Bi;
3) Extension of the isomer shift measurements both for the heavier ^{199,201,203}Bi and lighter ^{189,191}Bi isotopes;
4) Investigation of an inverse odd-even staggering in charge radii
   on the neutron-rich side for $^{214-218}$Bi.

ISOLDE RILIS laser system

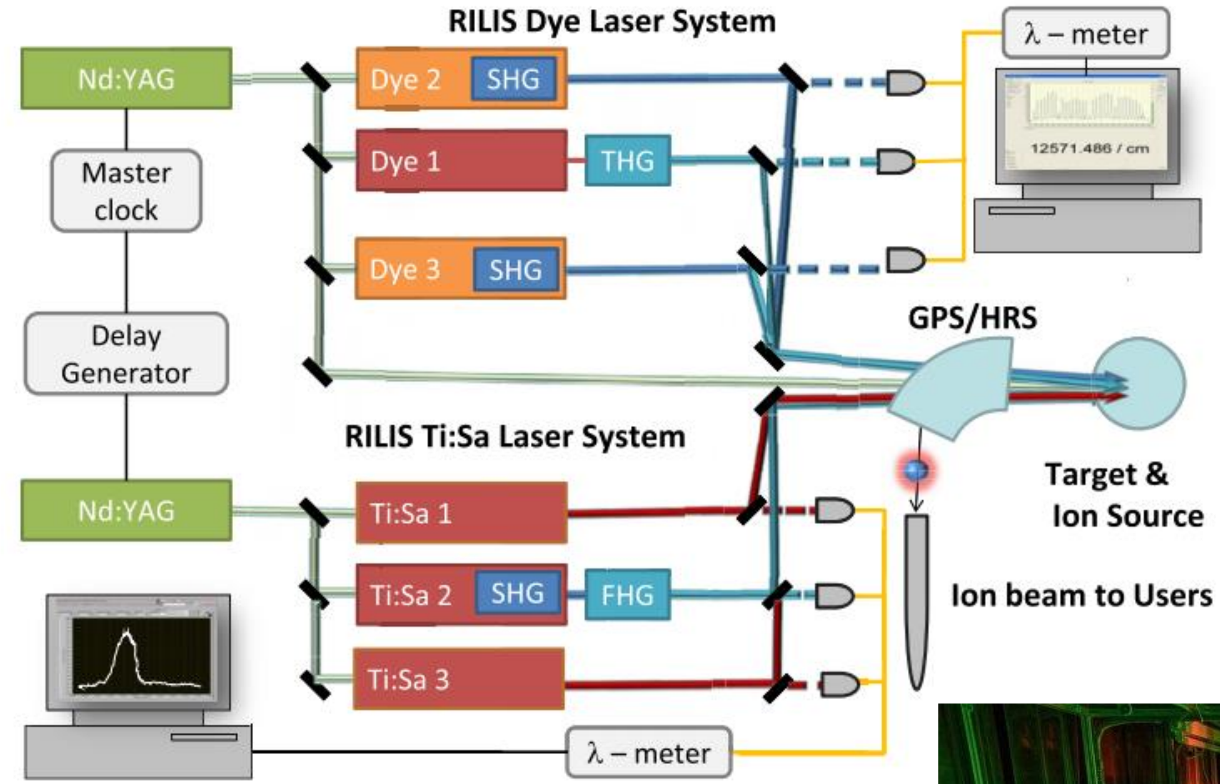

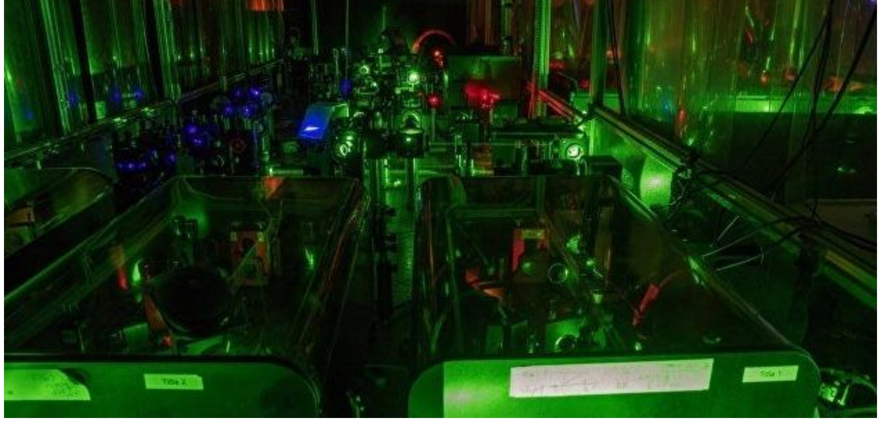

Positions of the hfs components on the spectrum

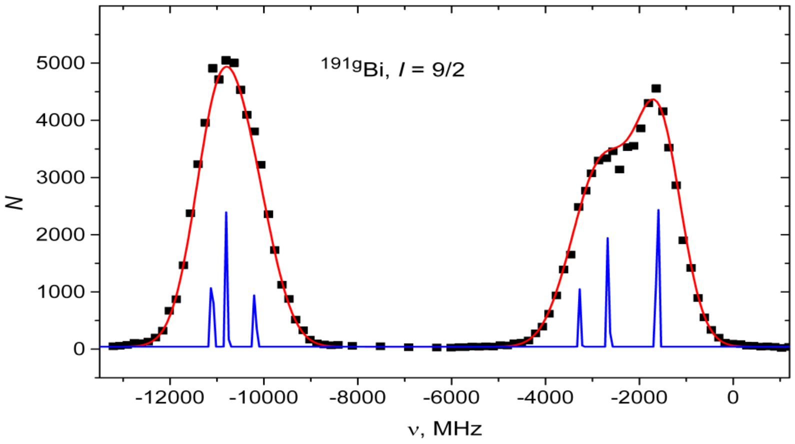

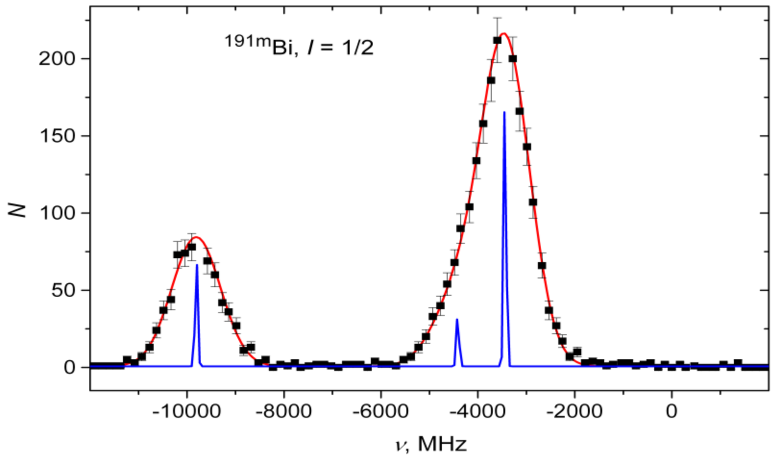

hyperfine structures for the states with nuclear spins *I* = 1/2 and *I* = 9/2 typical for neutron deficient Bi isotopes

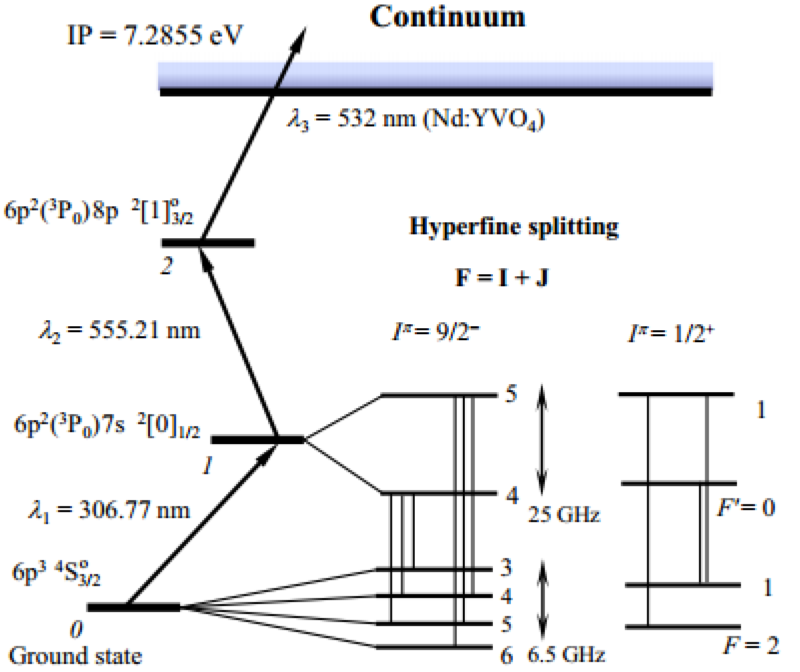

$$\nu_{F,F'} = \nu_0 + \Delta\nu_{F'} - \Delta\nu_F$$

ν_0 - the position of the center of gravity of the hfs,
the prime symbol denotes the upper level of the transition

$$\Delta\nu_F = a\cdot\frac{K}{2} + b\cdot\frac{0.75\cdot K\cdot(K+1) - I\cdot(I+1)\cdot J\cdot(J+1)}{2\cdot(2I-1)\cdot(2J-1)\cdot I\cdot J}$$

$$K = F\cdot(F+1) - I\cdot(I+1) - J\cdot(J+1)$$

$$\vec{F} = \vec{I} + \vec{J},\quad F = |I-J|, |I-J|+1, \ldots, I+J$$

$$a \propto \mu,\quad b \propto Q$$

IS608: Data analysis

$$\nu_{F,F'} = \nu_0 + \Delta\nu_{F'} - \Delta\nu_F$$

$$\Delta\nu_F = a\cdot\frac{K}{2} + b\cdot\frac{0.75\cdot K\cdot(K+1) - I\cdot(I+1)\cdot J\cdot(J+1)}{2\cdot(2I-1)\cdot(2J-1)\cdot I\cdot J}$$

$$K = F\cdot(F+1) - I\cdot(I+1) - J\cdot(J+1)$$

$$\vec{F} = \vec{I} + \vec{J},\quad F = |I-J|, |I-J|+1, \ldots, I+J$$

$$a \propto \mu,\quad b \propto Q$$

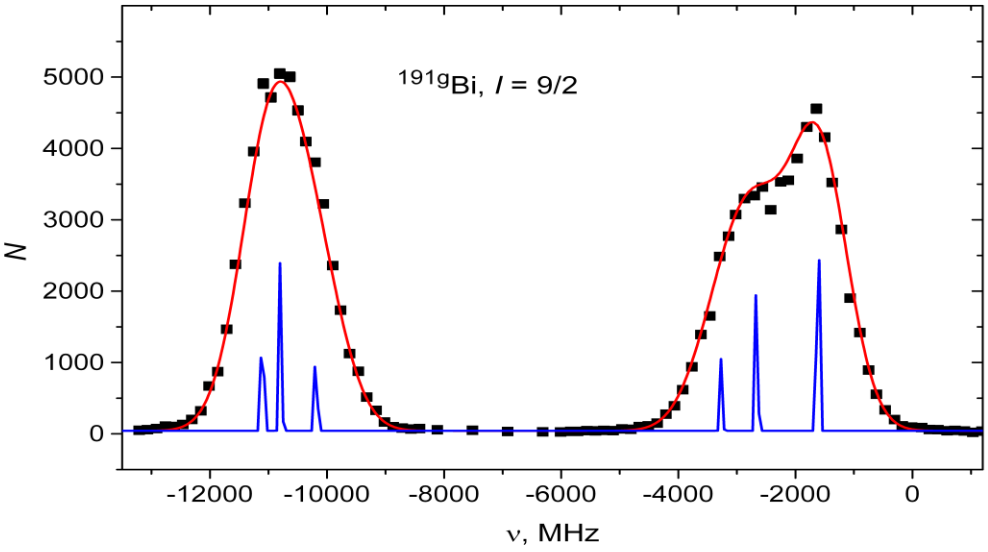

Free parameters for the fits:

relative IS to the stable ^{209}Bi (**$\delta\nu_{A,209}$**),

magnetic *hfs* constants (**a_1** and **a_2**),

electric quadrupole *hfs* constant (**b_1**)

The resolution of in-source RIS is limited by the Doppler broadening

$$\Delta\nu_D = 7.16 \times 10^{-7}\nu_0(T/A)^{1/2}$$

ν_0 - frequency of the atomic transition,
A - atomic mass number,
T – ionization temperature

IS608: nuclear moments

Nuclear magnetic moment μ_A: $$\mu_A = \mu_{209} \frac{I_A a_A(^4P_{1/2})}{I_{209} a_{209}(^4P_{1/2})} \left[1 + {}^{209}\Delta^A(^4P_{1/2})\right]$$

${}^{209}\Delta^A(^4P_{1/2})$ - relative hyperfine anomaly (**RHFA**) for the indicated atomic state

RHFA were estimated using data for heavier bismuth isotopes with the same spin and parity.

Spectroscopic quadrupole moment Q_s: $$\frac{Q_s(^A\mathrm{Bi})}{Q_s(^{209}\mathrm{Bi})} = \frac{b(^A\mathrm{Bi})}{b(^{209}\mathrm{Bi})}$$

$$b = eQ_s \times V$$

V - electric field gradient (EFG) produced by the electrons at the site of the nucleus

Independent Q_s measurements for ^{209}Bi made in the 1970s:
Q_s = –0.37(3) b (muonic x ray), Q_s = –0.50(8) b (pionic x ray)

The alternative way is:

- ✓ to calculate the EFG
- ✓ to deduce $Q_s(^{209}\mathrm{Bi})$ based on EFG and the measured $b(^{209}\mathrm{Bi})$

The complicated electronic structure makes accurate calculations for atomic bismuth a challenging problem

To overcome this longstanding discrepancy, we summarized the results of **33 atomic and molecular calculations** for ^{209}Bi, either published in the last decade (2013–2021) or made specifically for this study. In these calculations a variety of advanced theoretical methods with various computational strategies were used by several independent groups on **five continents**.

“world average” $Q_s(^{209}\mathrm{Bi})$ = -0.420(17) b

Nuclear Charge Radius and Isotope Shift (IS)

$\boxed{\delta\nu^{A,A'}} = \delta\nu_F^{A,A'} + \delta\nu_M^{A,A'}$ - isotope shift of optical line

$\delta\nu_F^{A,A'} = \boxed{F}\,\underline{\delta\langle r^2\rangle_{A,A'}}$ - mean-square charge radius

$$\delta\nu_M^{A,A'} = \frac{M(A-A')}{AA'}$$

$$M = M^{\mathrm{NMS}} + \boxed{M^{\mathrm{SMS}}}$$

🟨 - experiment

🟩 - calculations

The isotope shift contains a contribution from the difference in the mean square charge radius between the two isotopes but it is not always an easy task to extract this information

For bismuth isotopic chain advanced atomic calculations should be used for determination of electronic factor F and for evolution of specific mass shift constant M^{SMS}

hfs spectra of the selected Bi isotopes

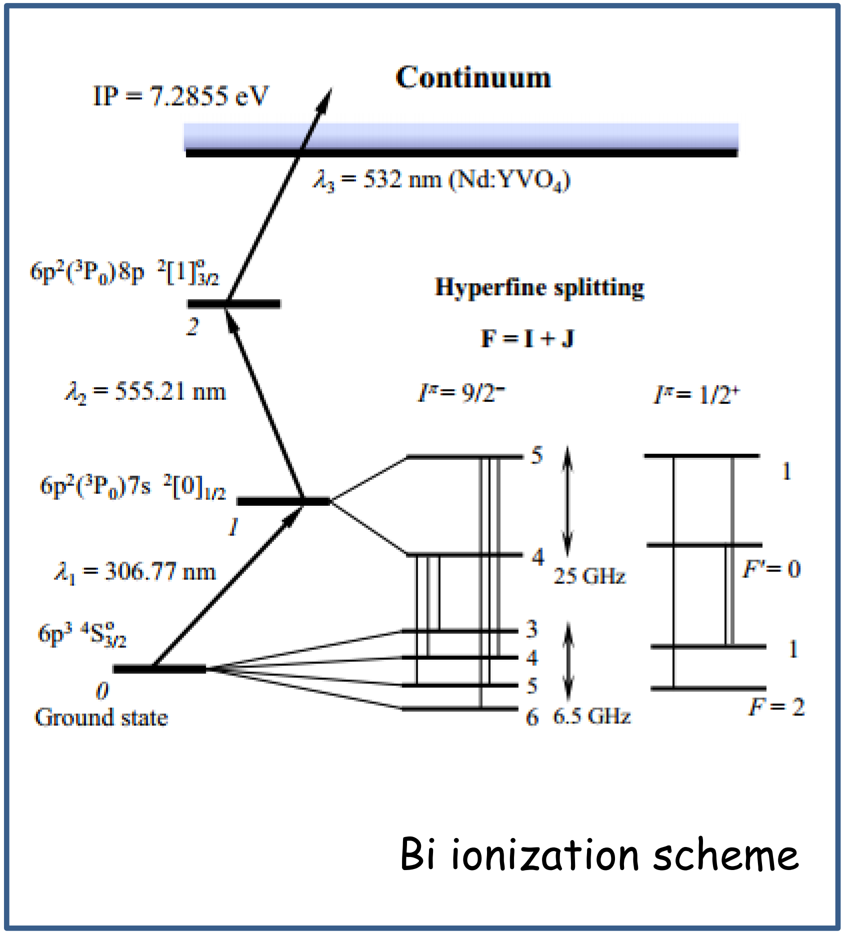

Bi ionization scheme

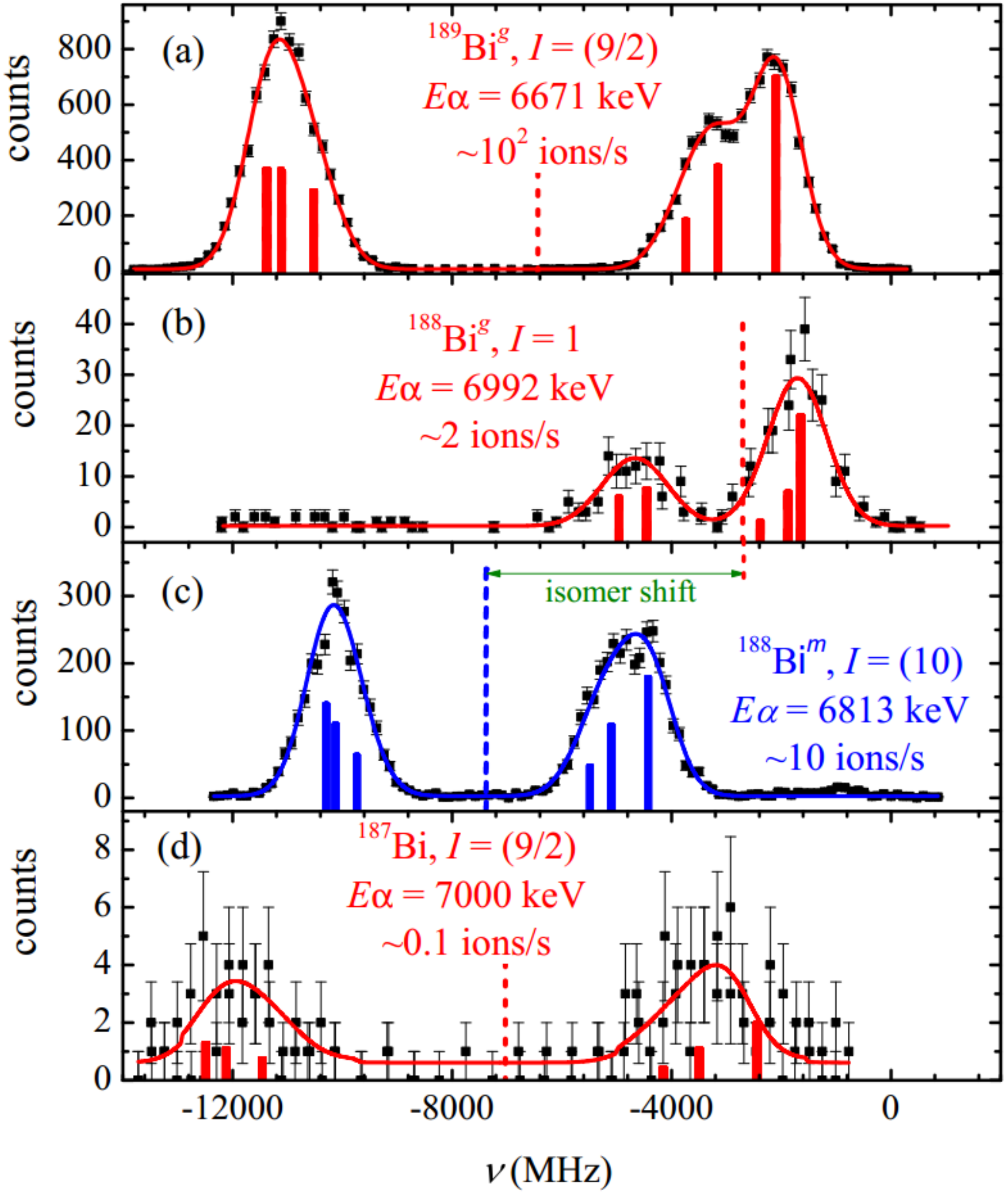

Shift of the centre of hfs gives isotope shift

Distance between peaks gives hfs splitting

Bi radii: 3 effects

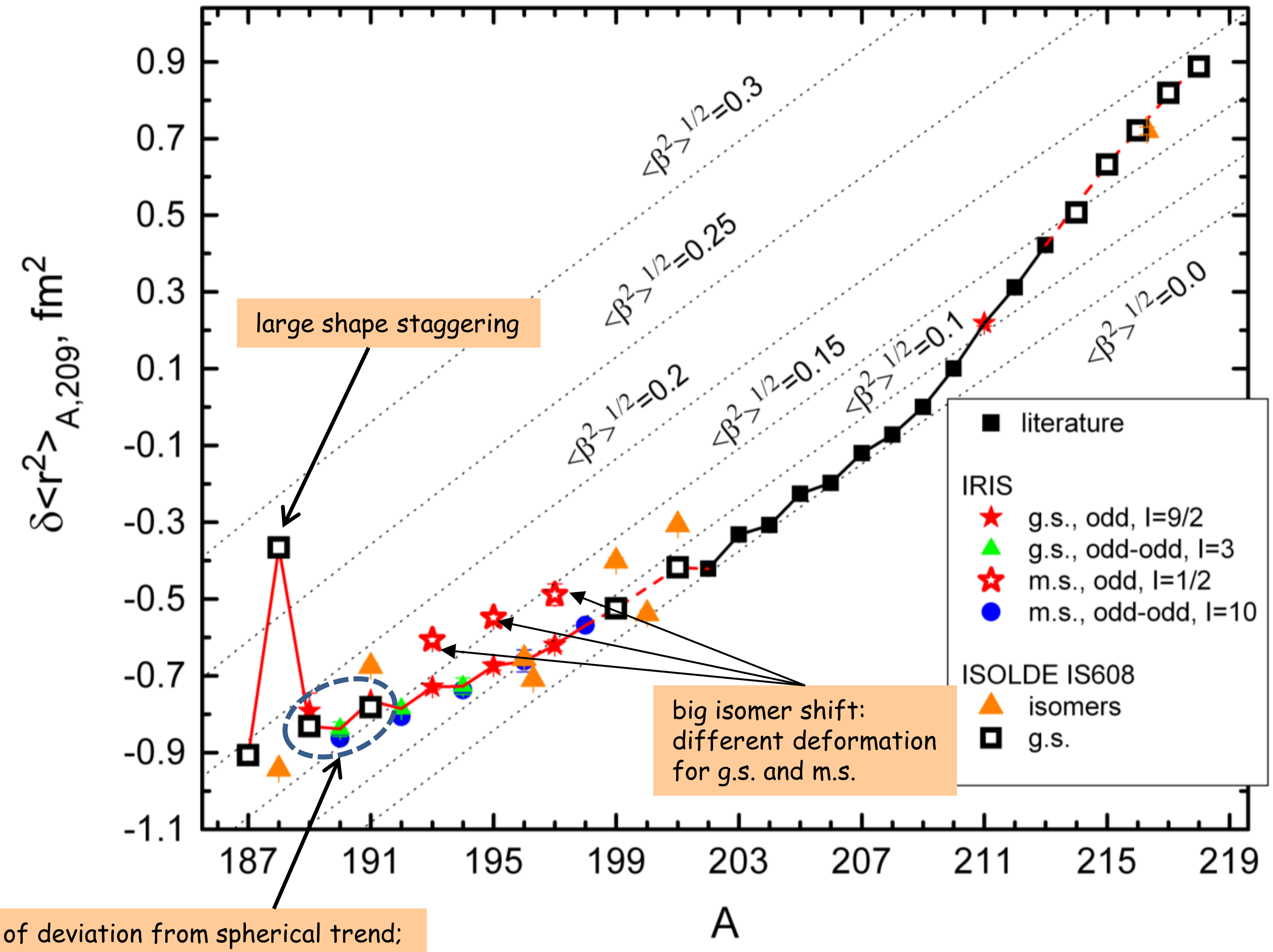

large shape staggering

big isomer shift:
different deformation
for g.s. and m.s.

start of deviation from spherical trend;
big odd-even staggering

$$\delta\left\langle r^2\right\rangle^{A,A'} = \delta\left\langle r^2\right\rangle_0^{A,A'} + \left\langle r^2\right\rangle_0 \cdot \frac{5}{4\pi}\delta\left\langle\beta_2^2\right\rangle^{A,A'}$$

Relative radii: Comparison of Tl, Pb and Po

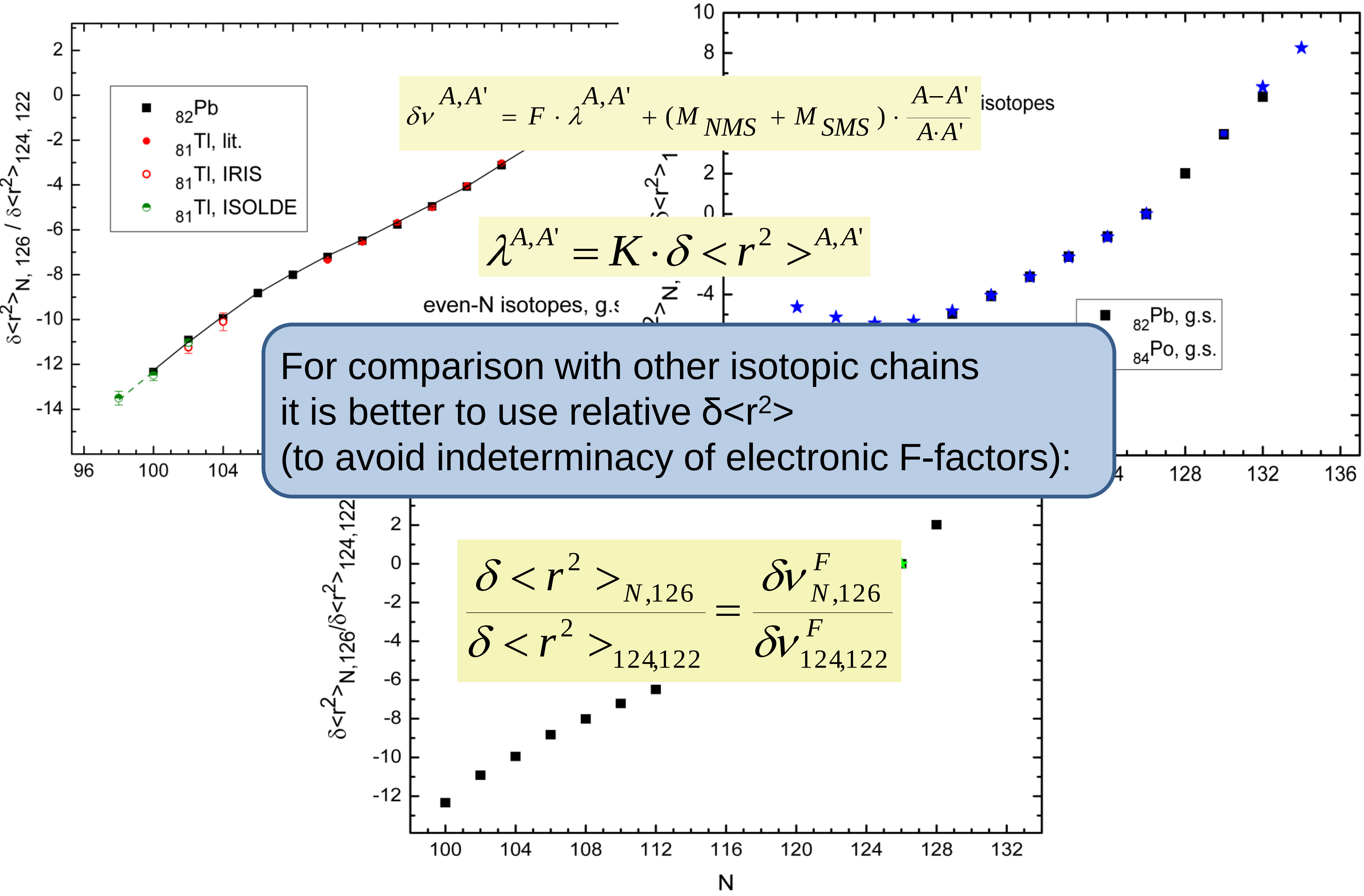

$$\delta\nu^{A,A'} = F \cdot \lambda^{A,A'} + (M_{NMS} + M_{SMS}) \cdot \frac{A-A'}{A \cdot A'}$$

$$\lambda^{A,A'} = K \cdot \delta < r^2 >^{A,A'}$$

For comparison with other isotopic chains
it is better to use relative δ<r²>
(to avoid indeterminacy of electronic F-factors):

$$\frac{\delta < r^2 >_{N,126}}{\delta < r^2 >_{124,122}} = \frac{\delta\nu^{F}_{N,126}}{\delta\nu^{F}_{124,122}}$$

Relative Bi radii: Deviation from spherical trend (Pb)

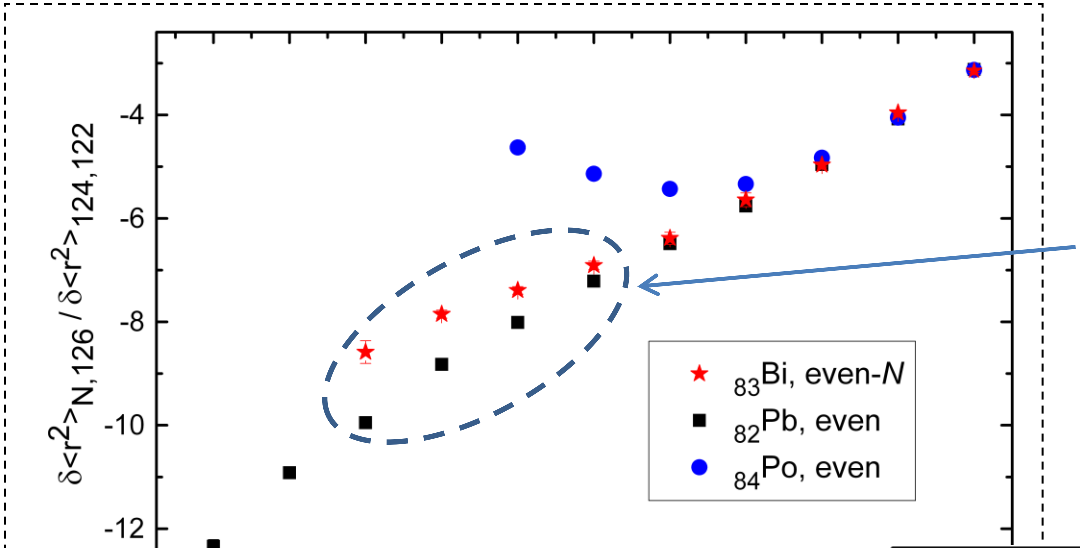

Marked deviation from the nearly spherical behavior for ground states of the even-neutron Bi isotopes at N < 111 in contrast to the Pb and Tl isotopic chains.

This deviation is interpreted as an indication of the onset of quadrupole deformation

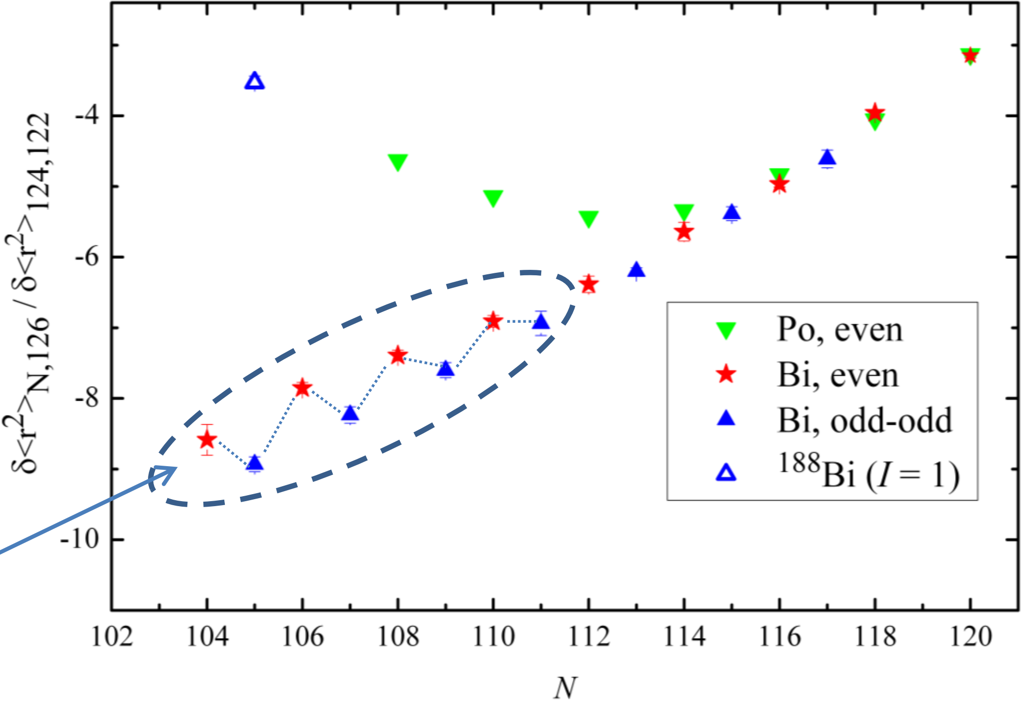

The deviation from the Pb-radii trend for the odd-neutron Bi isotopes is smaller than that for the even-neutron Bi isotopes.

This leads to the pronounced odd-even effect at N < 111

Bi & Hg: large shape staggering

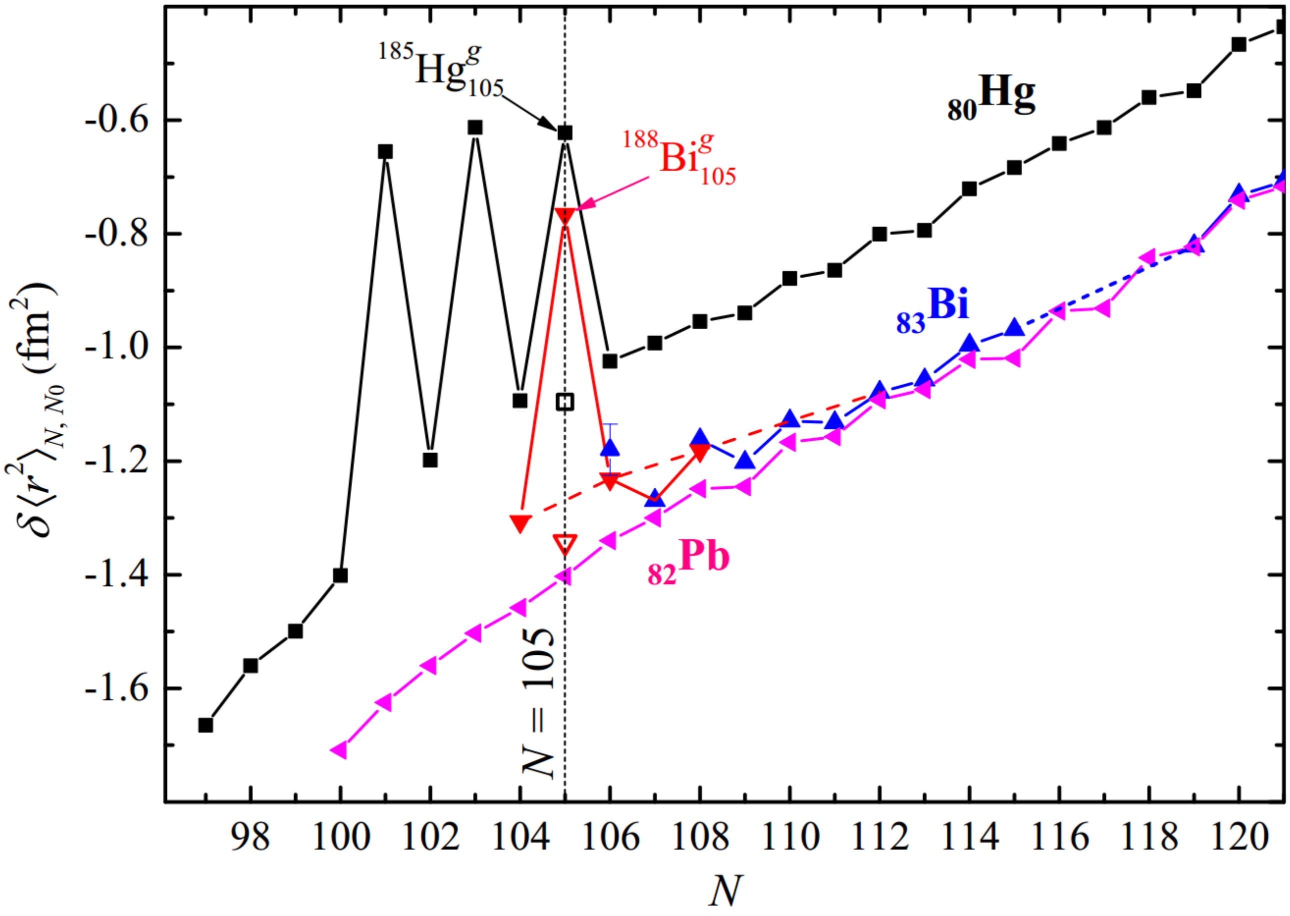

By performing laser-spectroscopy studies of $^{187-191}$Bi, we demonstrated a sharp radius increase for ^{188}Bi^{g}, relative to the neighboring ^{187,189}Bi^{g}.

Fifty years after discovery of shape-staggering in Hg, we have found only the second example of such an unusual behavior, now in the lightest Bi ($Z = 83$) isotopes with odd number of protons.

This dramatic change happens at the same neutron number ($N = 105$),
where the huge shape staggering started in the isotonic ^{185}Hg, and it has the same magnitude.

Comparison of β_Q and β_{DM}

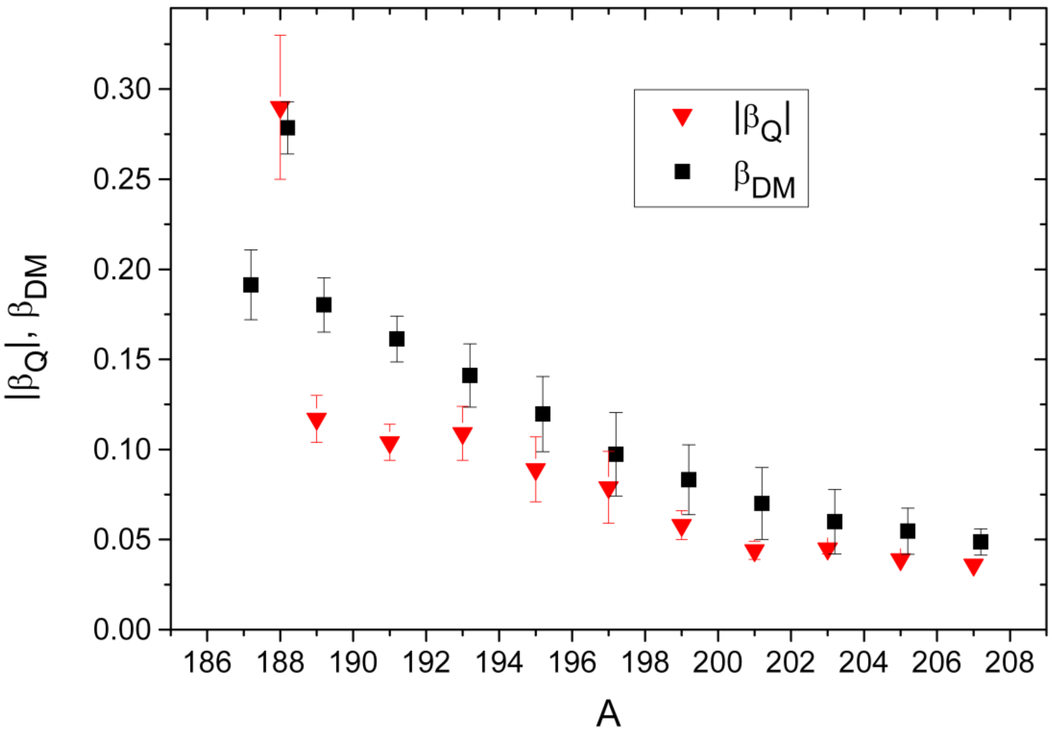

Influence of the nuclear deformation on changing of charge radii:

$$\delta\langle r^2\rangle^{A,A'} = \delta\langle r^2\rangle_0^{A,A'} + \langle r^2\rangle_0 \cdot \frac{5}{4\pi}\delta\langle\beta_2^2\rangle^{A,A'}$$

$$\beta_{DM} = \langle\beta_2^2\rangle^{1/2}$$

In the strong coupling scheme:

$$Q_s = \frac{I\cdot(2I-1)}{(I+1)\cdot(2I+3)} \cdot \frac{3e}{\sqrt{5\pi}} \cdot Z \cdot r_0^2 \cdot A^{2/3} \cdot \beta_Q \cdot \left(1 + \frac{1}{7}\cdot\sqrt{\frac{20}{\pi}}\cdot\beta_Q + \cdots\right)$$

In contrast to the mercury isotopes with spin 0 or 1/2 for which Qs ≡ 0, for ^{188}Bi^g one can directly check deformation using the measured Qs value.

Deformation parameter β_Q extracted from Q_s coincides with β_{DM} from $\delta\langle r^2\rangle$ and unambiguously testifies to the strong prolate deformation of ^{188}Bi^g

Radii in Pb-region: different shape evolution patterns

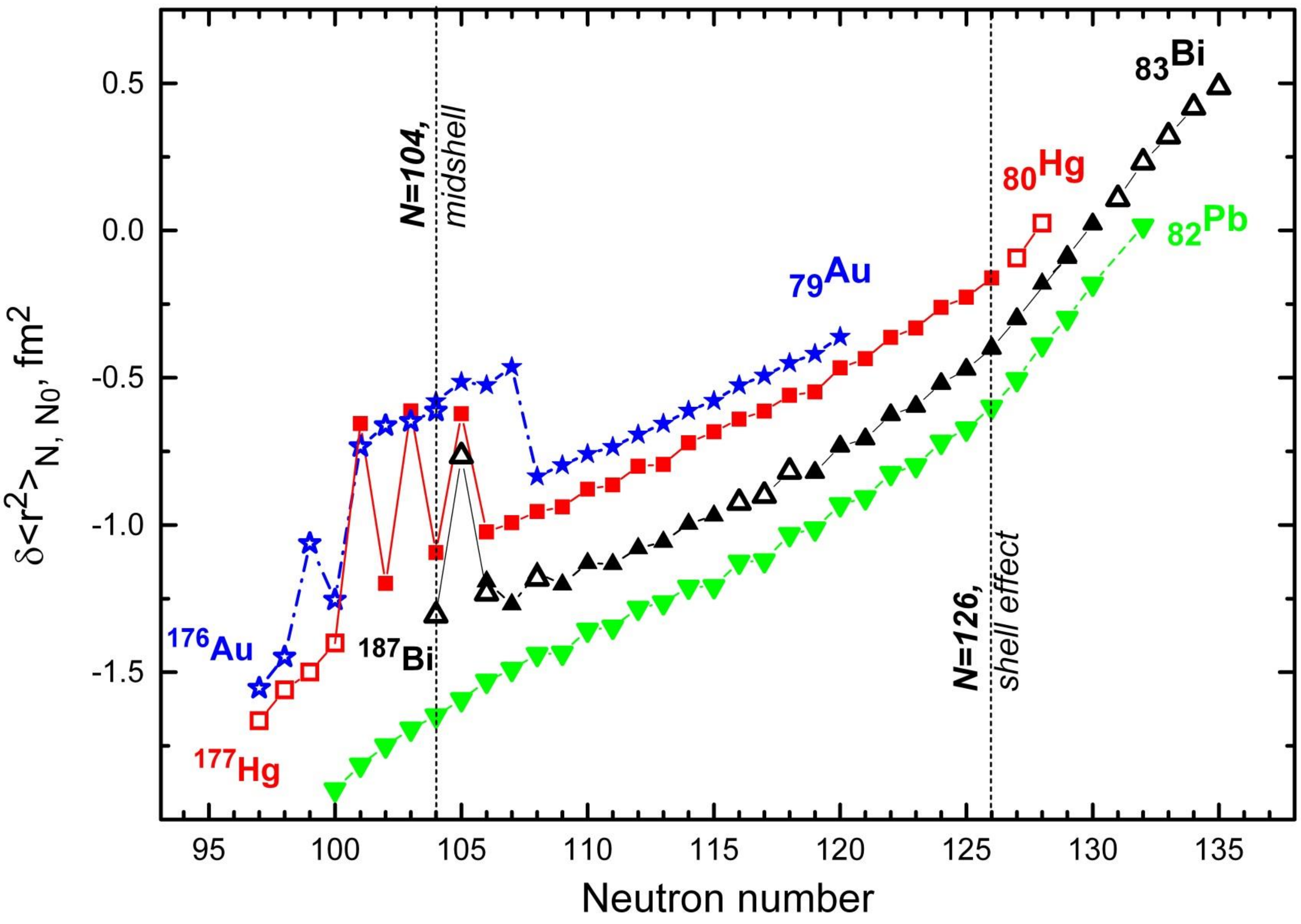

Large Shape Staggering in Neutron-Deficient Bi Isotopes

News · News · Topic: Physics

Voir en français

Bismuth isotopes also alternate from spheres to rugby balls

The unusual nuclear physics phenomenon, first discovered at CERN's ISOLDE facility 50 years ago, had until now been seen only in mercury isotopes

18 NOVEMBER, 2021 | By Ana Lopes

The ultrasensitive set-up used by the ISOLDE team to study bismuth isotopes. (Image: CERN)

Alternating from spheres to rugby balls is no longer the sole preserve of mercury isotopes, an international team at CERN's ISOLDE facility reports in a paper published in *Physical Review Letters*.

HFB calculation

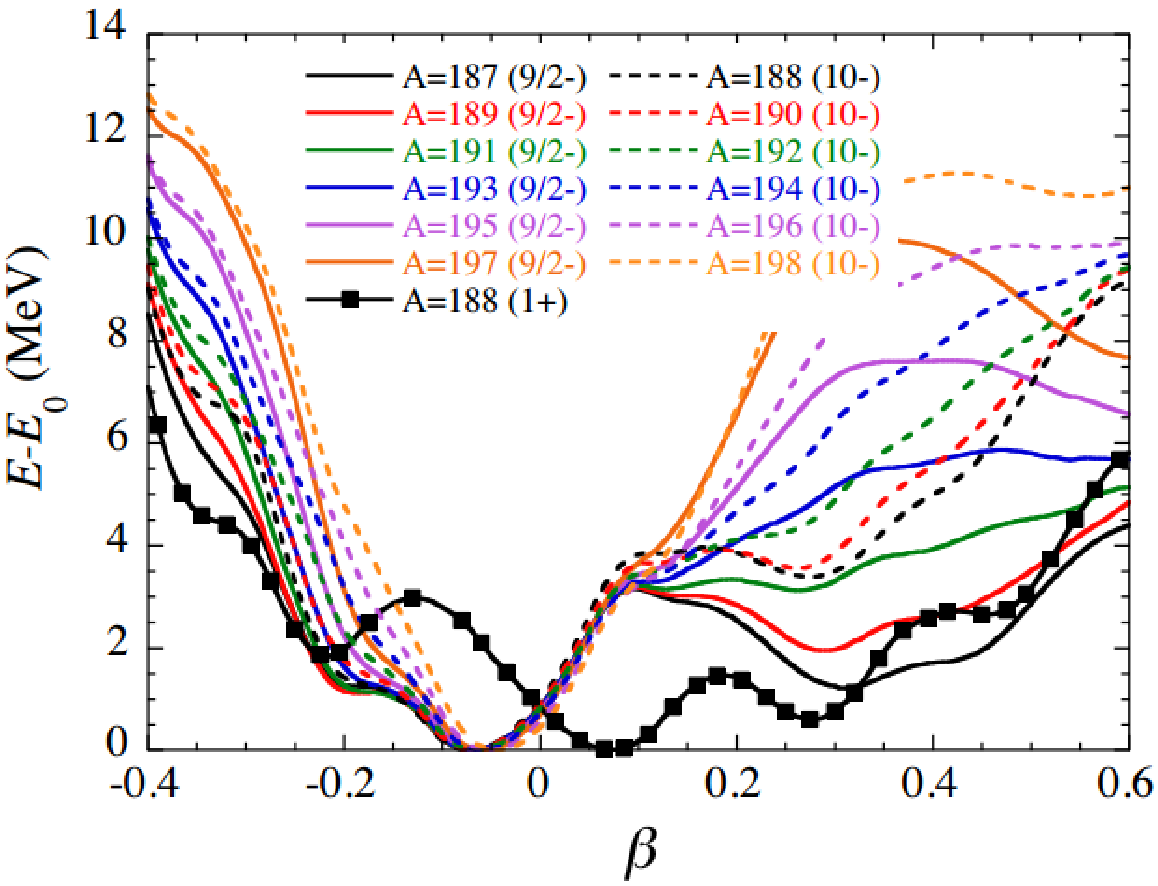

HFB PESs obtained by blocking the first $9/2^-$ qp in odd-A bismuth isotopes (solid lines), 10^- in even-A ones (dashed lines), and 1^+ in ^{188}Bi (squares). E_0 is the minimal energy of the corresponding PES. For each PES, at least one of the minima has a magnetic moment compatible with experimental data. For $9/2^-$ and 10^- states it is a minimum at $\beta \approx -0.07$, whereas for 1^+ state in ^{188}Bi it is a minimum at $\beta \approx +0.28$.

Bi: theory and experiment comparison

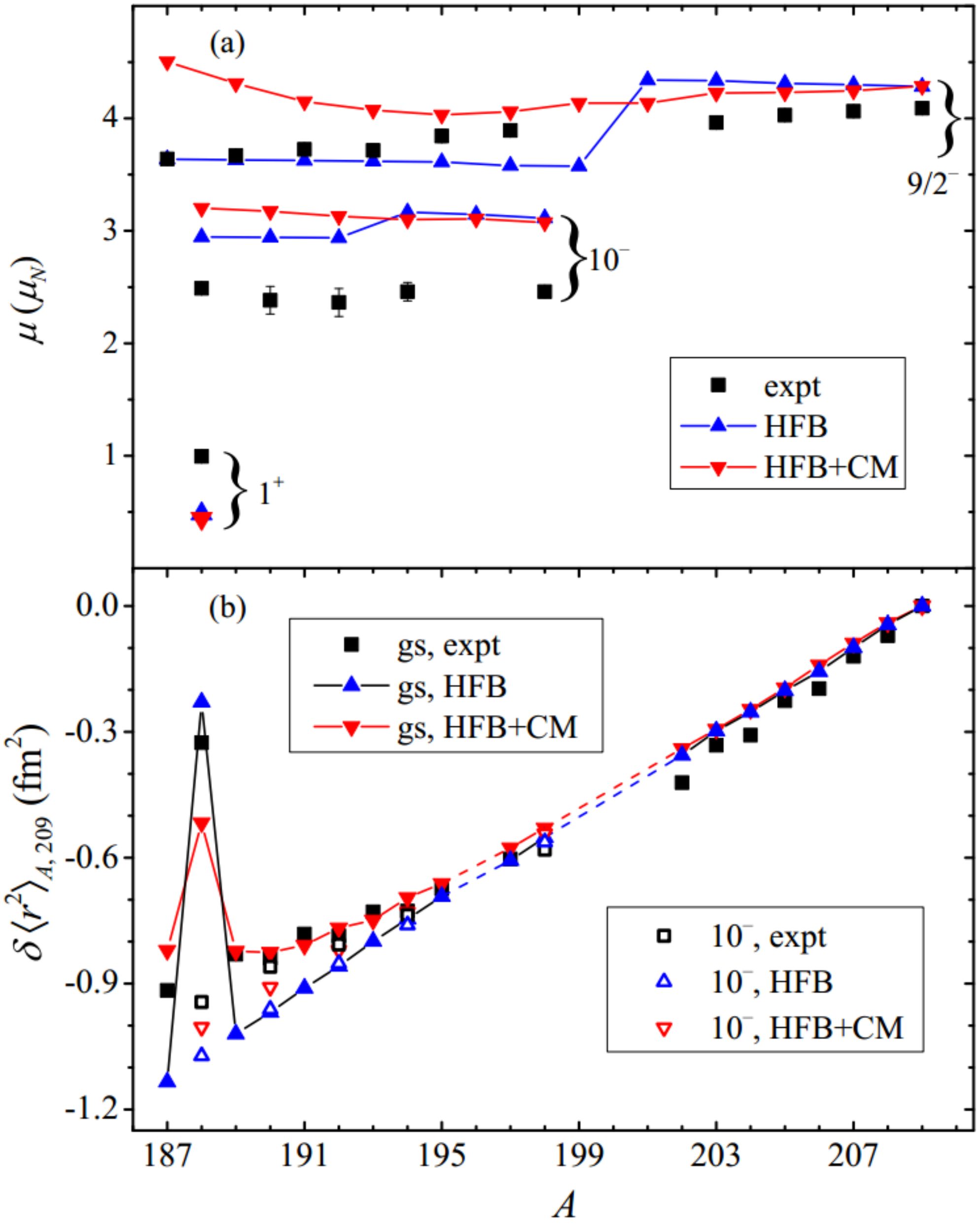

Shape staggering was successfully explained by HFB calculations, where the ground state is identified by the blocked quasiparticle configuration compatible with the observed spin, parity, and magnetic moment.

The departure from the trend for radii of Pb isotopes, found in light Bi's, was explained by invoking configuration mixing (CM) with states of different deformations.

CM for odd-A or odd-odd nuclei cannot currently be modeled microscopically.
Only future beyond-mean-field calculations will be able to shed light
on the exact impact of CM.

Conclusions

1. Laser ion source is very efficient tool for nuclear investigations due to its possibility to get the isobarically clean radioactive isotope beams of a great number of chemical elements.
2. Hyperfine structure parameters and isotope shifts of Bi isotopes relative to ^{209}Bi for the 306.9-nm atomic transition were measured using the in-source resonance-ionization spectroscopy technique at IRIS (PNPI) and ISOLDE (CERN). The changes in the mean-square charge radius, magnetic dipole and electric quadrupole moments were deduced using advanced atomic and molecular calculations.
3. A large staggering in radii was found near ^{188}Bi^{g}, along with the large isomer shift, at the same neutron number ($N = 105$), where the shape staggering starts and the similar isomer shift was observed in the mercury isotopes .
4. For the Bi nuclei the marked deviation from the isotopic trend of $\delta\langle r^2\rangle$ in the lead isotopic chains has been demonstrated at $N < 111$. This deviation has been interpreted as an indication of the onset of quadrupole deformation.